PRAMANA
— journal of
physics

Vol. 74, No. 2
February 2010
pp. 281–291

Temperature-dependent infrared reflectivity studies of multiferroic $TbMnO_3$: Evidence for spin-phonon coupling

PRADEEP KUMAR[1,*], SURAJIT SAHA[1], C R SERRAO[2,3], A K SOOD[1,3] and C N R RAO[3]

[1]Department of Physics, Indian Institute of Science, Bangalore 560 012, India
[2]Material Research Centre, Indian Institute of Science, Bangalore 560 012, India
[3]Chemistry and Physics of Materials Unit and International Centre for Materials Science, Jawaharlal Nehru Centre for Advanced Scientific Research, Bangalore 560 064, India
[*]Corresponding author.
E-mail: pkkhatri@physics.iisc.ernet.in (Pradeep Kumar);
asood@physics.iisc.ernet.in (A K Sood)

MS received 24 June 2009; revised 12 September 2009; accepted 15 September 2009

Abstract. We have measured near normal incidence far-infrared (FIR) reflectivity spectra of a single crystal of $TbMnO_3$ from 10 K to 300 K in the spectral range of 50 cm^{-1}–700 cm^{-1}. Fifteen transverse optic (TO) and longitudinal optic (LO) modes are identified in the imaginary part of the dielectric function $\varepsilon_2(\omega)$ and energy loss function $\mathrm{Im}(-1/\varepsilon(\omega))$, respectively. Some of the observed phonon modes show anomalous softening below the magnetic transition temperature T_N (∼46 K). We attribute this anomalous softening to the spin-phonon coupling caused by phonon modulation of the superexchange integral between the Mn^{3+} spins. The effective charge of oxygen (Z_O) calculated using the measured LO–TO splitting increases below T_N.

Keywords. Spin-phonon coupling; longitudinal and transverse optic modes; effective charge; energy loss function.

PACS Nos 78.30.j; 75.47.lx; 63.20.kk

1. Introduction

Multiferroics are materials in which electric and magnetic properties are correlated. These materials have attracted much attention in recent years because of their magnetoelectric phenomena as well as potential applications [1–4]. Only a few systems with strong magnetoelectric effect are known because proper ferroelectricity and magnetism tend to be mutually exclusive and interact very weakly whenever they coexist [5]. Much of the recent interest is in systems with improper ferroelectricity, which is due to the exchange striction in magnetically ordered states [1] and this

produces strong coupling between magnetic and ferroelectric order parameters. A strong coupling between spin, charge and lattice degrees of freedom in perovskite manganite, $R\mathrm{MnO_3}$ (R = rare earth), gives many competing phases. An identification of large magnetoelectric and magnetocapacitive effects in undoped perovskite manganites with small-sized R cations, e.g., $\mathrm{TbMnO_3}$ and $\mathrm{DyMnO_3}$, has made the family of manganites even more interesting [6,7]. It has been shown that an external electric field can change the magnetic domain distribution [8]. Depending on the size of the R-ion, these materials have two kinds of crystal structure. $R\mathrm{MnO_3}$ crystallize in orthorhombic structure for R with larger ionic radius (R = La, Ce, Pr, Nd, Sm, Eu, Gd, Tb and Dy) and in hexagonal structure for R with smaller ionic radius (R = Ho, Er, Tm, Yb, Lu, Y). All the $R\mathrm{MnO_3}$ perovskites show a distortion of $\mathrm{MnO_6}$ octahedra due to the Jahn–Teller (JT) effect of $\mathrm{Mn^{3+}}$ cations [9–11]. At room temperature, $R\mathrm{MnO_3}$ shows paramagnetic and insulating behaviour. The latter arises from splitting of the e_g level of the d-electrons of the Mn-ions, caused by the JT distortion of the $\mathrm{MnO_6}$ octahedra.

$\mathrm{TbMnO_3}$ is orthorhombic (space group Pbnm) at room temperature and shows an incommensurate lattice modulation at T_N for sinusoidal antiferromagnetic ordering, with $T_\mathrm{N} \sim 41$ K [6] or $T_\mathrm{N} \sim 46$ K as reported by Bastjan *et al* [12]. Ferroelectric order develops at the incommensurate–commensurate transition temperature $T_\mathrm{FE} \sim$27 K [6]. The lattice modulation below T_N is caused by the $\mathrm{Mn^{3+}}$ ions increasing their exchange interaction energy by shifting their positions [13,14]. It has been suggested that the origin of ferroelectricity in $\mathrm{TbMnO_3}$ is induced by the complex spin structure [7]. As the temperature is further lowered, rare-earth $\mathrm{Tb^{3+}}$ ions also order antiferromagnetically in $\mathrm{TbMnO_3}$ at $T \sim 7$ K [6].

The role of phonons in manganites has been studied in recent years using Raman and infrared spectroscopies. In recent years, focus has been on the electromagnons observed below 150 $\mathrm{cm^{-1}}$ [15–19]. Electromagnons are the spin waves that are excited by an AC electric field. These electromagnons are qualitatively different from the spin-phonon coupling. It has been shown that in $R\mathrm{MnO_3}$ (R = La, Nd, Sm, Gd, Dy and Pr), a few Raman phonons involving oxygen vibrations are anomalous, i.e. the phonon frequency decreases as temperature is lowered below T_N [20–22] and this is attributed to spin-phonon coupling. However, there have not been detailed temperature-dependent studies on infrared (IR) phonons in $R\mathrm{MnO_3}$, except the work of Paolone *et al* [23] wherein they have reported IR mode frequencies at 300 K and 10 K for undoped and doped $\mathrm{LaMnO_3}$. From their tabulated data, it is seen that three modes in undoped and one mode in doped samples show lower frequencies at 10 K as compared to their values at 300 K. In this paper, we report a detailed temperature-dependent study of infrared phonons in $\mathrm{TbMnO_3}$ in the 10–300 K range.

2. Experimental details

A floating-zone furnace fitted with two ellipsoid halogen lamps (NEC-Japan) with radiation heating was used to grow single crystals of $\mathrm{TbMnO_3}$. Polycrystalline rods (feed and seed) were prepared by conventional solid-state reaction method. Stoichiometric mixtures of the starting materials $\mathrm{Tb_2O_3}$ and $\mathrm{MnO_2}$ were weighed in the

desired proportions and grounded for a few hours in an agate mortar with propanol. The powder is heated at 1173 K, 1273 K, 1473 K with intermediate grinding. The powder was finally sintered at 1673 K for 24 h in air. The sample was then re-grounded and monophasic polycrystalline powder was hydrostatically pressed and sintered at 1473 K for 24 h in air to obtain the feed and seed rods with a diameter of 4 mm and a length of 100 mm. A single crystal was then grown under an air atmosphere at a growth rate of 6 mm/h.

Reflectance spectra of the unoriented $TbMnO_3$ single crystal were obtained in near-normal incidence geometry using a Fourier transform IR spectrometer (Bruker IFS 66v/s) in the frequency range of 50–700 cm^{-1}. The noise level below 150 cm^{-1} did not allow us to study electromagnons in our experiment. We will focus on the temperature dependence of the infrared active phonons with frequencies above 150 cm^{-1}. Spectra were collected with an instrumental resolution of 2 cm^{-1}. The background reference signal was collected using a gold plated mirror. Temperature-dependent reflectance spectra at temperatures ranging from 10 K to 300 K were collected by mounting the sample on the cold finger of a continuous flow liquid helium cryostat (Optistat CF-V, Oxford Instruments) and the temperature was controlled to an accuracy of ±0.1 K by a temperature controller (Oxford Instruments).

3. Results and discussion

The temperature-dependent reflectivity of $TbMnO_3$ is shown in figure 1 for a few typical temperatures. The bands in the reflectivity spectra are due to IR active phonon modes. The total numbers of IR active phonon modes of $TbMnO_3$ (space group: Pbnm), calculated using group theory are 25 and these are classified as $\Gamma_{IR} = 9B_{1u} + 7B_{2u} + 9B_{3u}$ [22]. The eigenvectors of these modes have been reported [24] using rigid ion model. The dielectric function, $\varepsilon(\omega)$, was obtained by Kramer–Kronig (KK) analysis of the reflectance spectra using the OPUS software (Bruker Optics). The extrapolation procedure used in KK analysis was as follows: reflectivity value $R(\omega)$ below 50 cm^{-1} is the same as R (50 cm^{-1}) and R (ω >700 cm^{-1}) = $R(\omega = 700\ cm^{-1})$. Peak positions in the imaginary part of the dielectric function ($\varepsilon_2(\omega)$) and energy loss function ($\mathrm{Im}(-1/\varepsilon(\omega))$) give the frequencies of the transverse optic (TO) and longitudinal optic (LO) modes, respectively. Temperature-dependent $\varepsilon_2(\omega)$ shown in figure 2 for a few typical temperatures clearly reveal 15 TO modes, labelled as T1 to T15, apart from some weak modes which appear as shoulders (not labelled). It is likely that the band labelled as T3 can be a combination of two modes, as indicated by its lineshape at low temperatures. The corresponding LO modes identified as L1 to L15 in $\mathrm{Im}(-1/\varepsilon(\omega))$, are shown in figure 3 for a few typical temperatures. We tried to fit $\varepsilon_2(\omega)$ and $\mathrm{Im}(-1/\varepsilon(\omega))$ by a sum of 15 Lorentizian-like functions [25,26] to extract the peak positions, linewidth and oscillator strengths of the IR modes. This could not be done due to large number of parameters (15×3 + one for $\varepsilon(\infty)$ + base line parameter = 47). We, therefore, have extracted only the peak positions by directly reading from the spectra of $\varepsilon_2(\omega)$ and $\mathrm{Im}(-1/\varepsilon(\omega))$. These values are given in table 1 for 300 K to give an indication of the LO–TO splitting in $TbMnO_3$. The mode

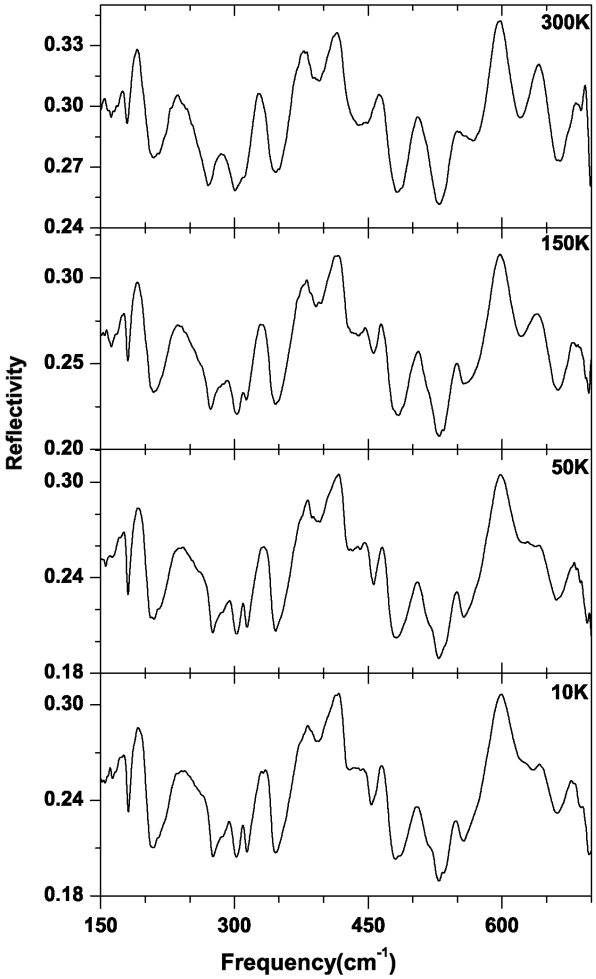

Figure 1. Temperature-dependent infrared reflectivity of $TbMnO_3$ in the spectral range 150–700 cm^{-1}.

frequencies are close to the observed [23] and calculated [24] frequencies for the infrared phonons of $LaMnO_3$.

We will now discuss the temperature dependence of the LO and TO modes extracted from the reflectivity measurements. It is seen that the temperature-dependence of nine modes (modes 1–3, 7, 9, 10, 11, 14 and 15) is very weak and normal (data not shown), i.e. the mode frequency increases by less than 1 or 2 cm^{-1} as temperature is lowered to 10 K. Figures 4 and 5 show the temperature dependence of other modes 4, 5, 6, 8, 12 and 13 for both the LO and TO components which reveal significant temperature dependence.

In general, the temperature-dependent behaviour of a phonon mode of frequency ω is given as [21]

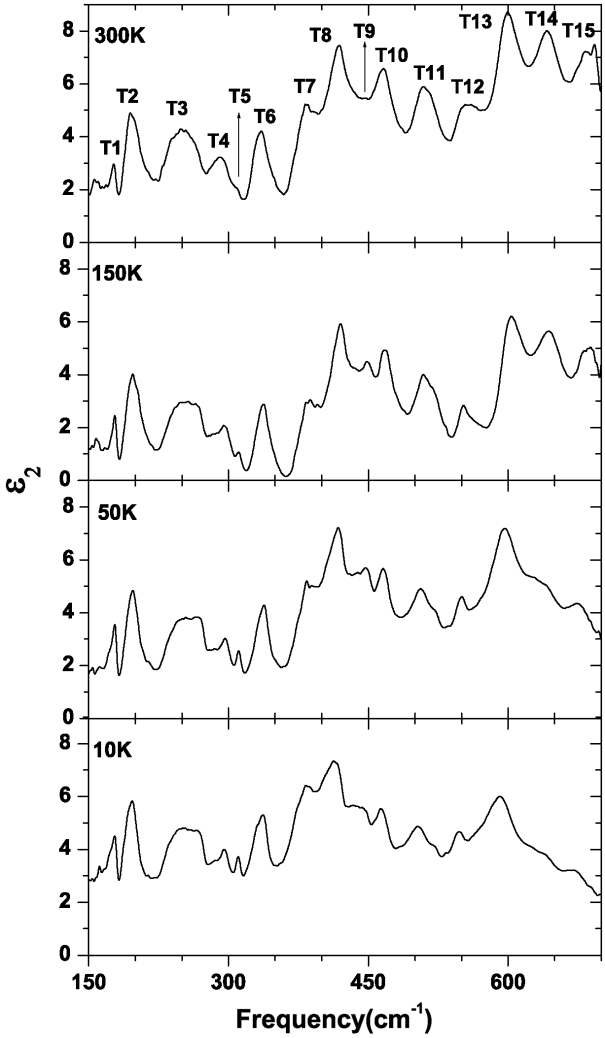

Figure 2. Temperature dependence of the imaginary part of the dielectric function ($\varepsilon_2(\omega)$).

$$\omega(T) = \omega(0) + (\Delta\omega)_{\rm qh}(T) + (\Delta\omega)_{\rm anh}(T) + (\Delta\omega)_{\rm el-ph}(T) + (\Delta\omega)_{\rm sp-ph}(T), \quad (1)$$

where $\omega(0)$ is the phonon frequency at $T = 0$ K. The term $(\Delta\omega)_{\rm qh}(T)$ corresponds to the change in phonon frequency due to a change in the unit cell volume, termed as quasiharmonic effect. $\Delta\omega_{\rm anh}(T)$ represents the intrinsic anharmonic contributions to the phonon frequency, which is related to the real part of the phonon self-energy. The effect of renormalization of the phonon frequency ($(\Delta\omega)_{\rm el-ph}(T)$) due to electron–phonon coupling is absent in insulating $TbMnO_3$. The term $\Delta\omega_{\rm sp-ph}(T)$ is the change in phonon frequency due to spin-phonon

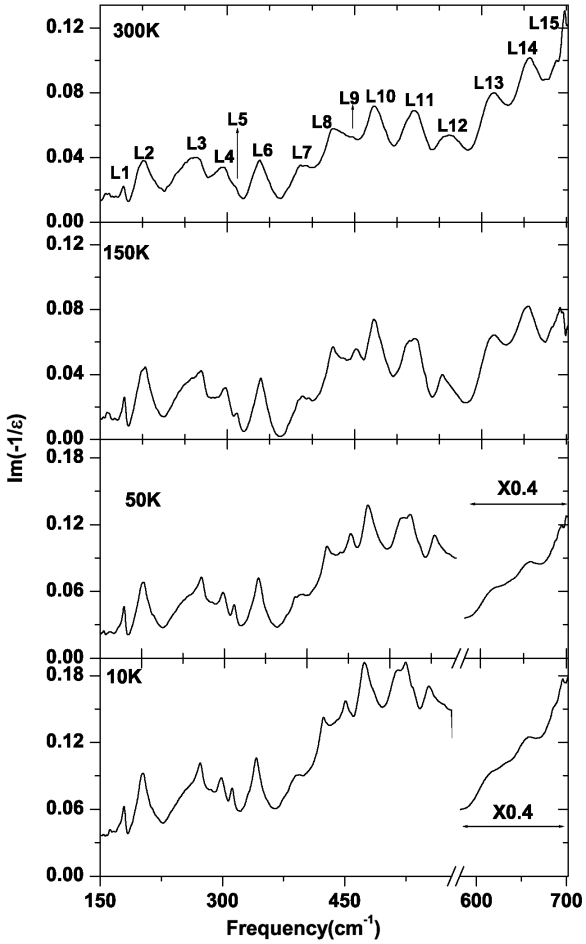

Figure 3. Evolution of the energy loss function ($\mathrm{Im}(-1/\varepsilon(\omega))$) with temperature.

coupling, caused by the modulation of the exchange integral by lattice vibrations [21]. The change in phonon frequency of mode i due to change in lattice constant, i.e. $(\Delta\omega)_{\mathrm{qh}}(T)$, can be related to the change in volume if we know Grüneisen parameter $\gamma_i = -(B_0/\omega_i)(\partial\omega_i/\partial P)$, where B_0 is the bulk modulus and $\partial\omega_i/\partial P$ is the pressure derivative of the phonon frequency. For a cubic crystal or isotropically expanded lattice, the change in phonon frequency due to change in volume is given as $(\Delta\omega)_i(T)_{\mathrm{qh}}/\omega_i(0) = -\gamma_i(\Delta V(T)/V(0))$. In the Raman study of $R\mathrm{MnO_3}$ (R = Gd, Eu, Pr, Nd, Sm, Tb, Dy, Ho and Y), the quasiharmonic contribution has been neglected [20,22]. Similarly, the quasiharmonic contribution in $\mathrm{TbMnO_3}$ can also be neglected because the coefficient of thermal expansion for the lattice parameter c remains nearly constant whereas for a and b it varies in opposite direction [27]. Therefore, fractional change in volume is negligible and hence $(\Delta\omega_i)_{\mathrm{qh}}(T)$ can be ignored.

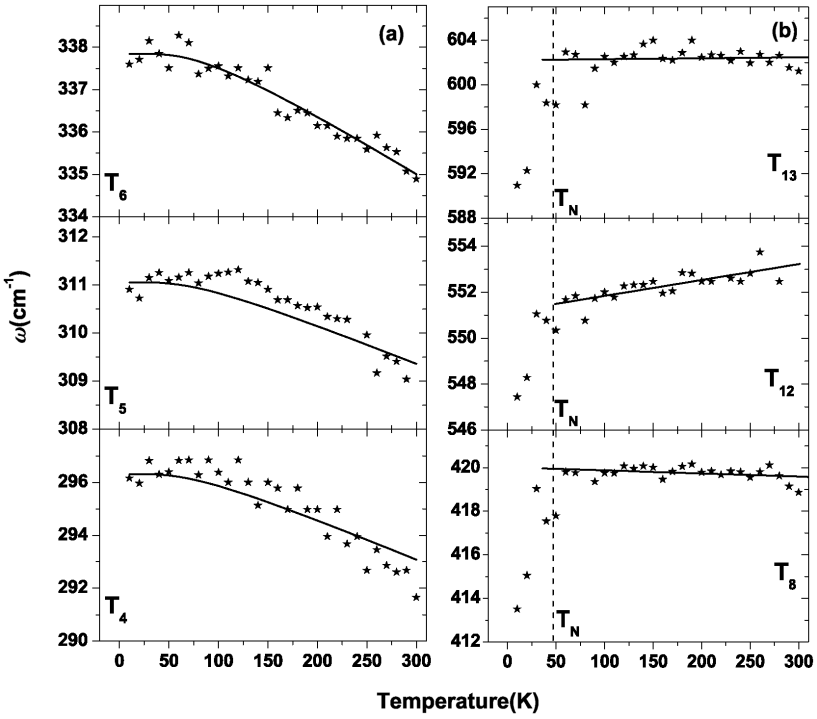

Figure 4. Temperature dependence of the TO modes T4, T5, T6, T8, T12 and T13. Solid lines for T4, T5 and T6 are the fitted curves as described in the text. The frequencies for the T8, T12 and T13 modes have been fitted by a linear relation above T_{N}.

In a cubic anharmonic process, a phonon of frequency $\omega(\vec{\kappa} = 0)$ decays into two phonons $\omega_1(\vec{\kappa}_1)$ and $\omega_2(\vec{\kappa}_2)$, keeping energy and momentum conserved, i.e. $\omega = \omega_1 + \omega_2$, $\vec{\kappa}_1 + \vec{\kappa}_2 = 0$. Considering the simplest decay channel with $\omega_1 = \omega_2$, the temperature dependence of $\omega(T)$ can be expressed as [28]

$$\omega(T) = \omega(0) + C[1 + 2n(\omega(0)/2)], \tag{2}$$

where $\omega(T)$ is the phonon frequency at temperature T, $\omega(0)$ is the phonon frequency at $T = 0$ K in the harmonic approximation, C is the self-energy parameter for a given phonon mode and $n(\omega) = 1/(\exp(\hbar\omega/\kappa_{\mathrm{B}}T) - 1)$ is the Bose–Einstein mean occupation number. We have fitted the modes T4, T5, T6; L4, L5, L6 and L13 using eq. (2). The solid lines, in figures 4 and 5, correspond to the fits by eq. (2), with fitting parameters given in table 1.

The most interesting observation from our experiments is that the modes T8, T12, T13 (figure 4) and L12 (figure 5) show anomalous temperature dependence: the modes show softening below T_{N}. Similar anomalous temperature dependence has been observed for a few Raman modes in $R\mathrm{MnO_3}$ where R = La [16] and Gd, Pr, Nd, Sm, Dy [20,22], which has been attributed to spin-phonon coupling [21]. This is understood as follows: if an ion is displaced from its equilibrium position by

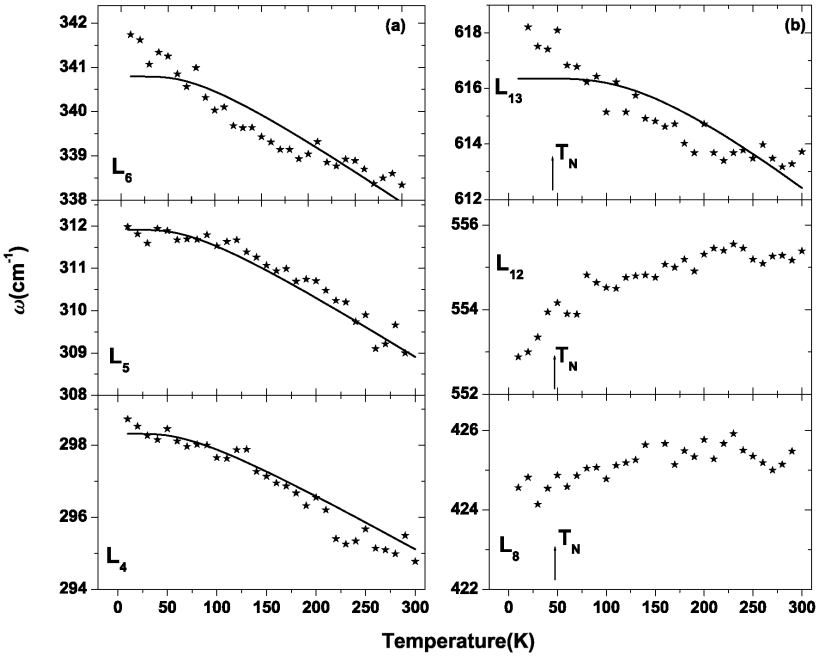

Figure 5. Temperature evolution of the LO modes L4, L5, L6, L8, L12 and L13. Solid lines for L4, L5, L6 and L13 are the fitted curves as described in the text.

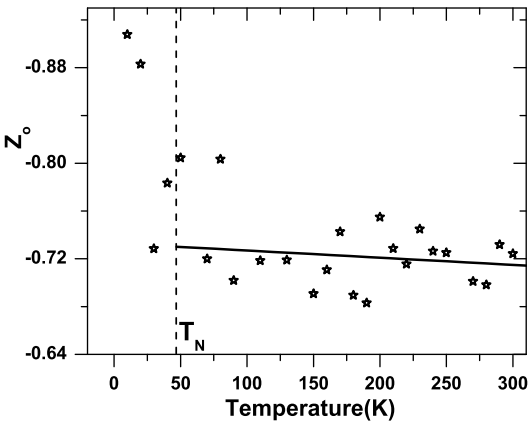

Figure 6. Temperature dependence of the effective charge of oxygen (Z_{O}). Solid line shows a linear fit in the temperature range above T_{N}.

u, then the crystal potential is given as $U = (1/2)(ku^2) + \Sigma_{ij} J_{ij}(u) S_i S_j$, where k in the first term represents the force constant and the second term arises from spin interactions between the Mn^{3+} spins; second derivative of the crystal potential (U) gives a harmonic force constant. The phonon frequency is affected by the additional

Table 1. List of the experimental phonon frequencies at 300 K and fitting parameters of a few phonons, fitted by eq. (2) as described in text. Units are in cm^{-1}.

Mode label number	TO mode frequency			LO mode frequency		
	$\omega(300)$	$\omega(0)$	C	$\omega(300)$	$\omega(0)$	C
1	176			177		
2	197			201		
3	252			260		
4	291	298.2±0.9	−3.4±1.4	295	300.6±0.4	−3.1±1.2
5	309	312.4±1.1	−2.7±0.6	309	313.6±1.2	−2.1±0.8
6	335	339.6±1.3	−3.6±1.4	338	342.6±0.4	−3.5±0.8
7	384			387		
8	419			425		
9	446			449		
10	465			474		
11	511			520		
12	552			555		
13	601			614	623.2±1.1	−3.6±0.9
14	641			657		
15	686			697		

term, i.e. $(\Delta\omega)_{\mathrm{sp-ph}}(T) = \lambda\langle S_i S_j\rangle$, where $\lambda = (\partial^2 J_{ij}(u)/\partial u^2)$ is the spin-phonon coupling coefficient and $\langle S_i S_j\rangle$ is the spin correlation function. λ can be positive or negative and is different for different phonons. As the temperature decreases, the spin correlations build up and hence the spin-phonon coupling becomes important at lower temperatures. Therefore, renormalization of the phonon frequency below T_N is expected in $TbMnO_3$. We note that the phonon softening for the T13 mode is similar in magnitude to the B_{2g} ($\sim$604 cm^{-1}) mode in $LaMnO_3$ [21] and hence the spin-phonon coupling constant (λ) is expected to be similar for both the modes.

We now comment on the temperature dependence of the frequency difference between the LO and TO modes which determines the effective charge of the ions in the lattice. The effective charge of Tb, Mn and O ions in the unit cell with k atoms can be estimated using the relation [29]

$$\Sigma_k(Z_k^2/M_k) = (\pi V)\Sigma_j(\omega_{\mathrm{LO},j}^2 - \omega_{\mathrm{TO},j}^2), \tag{3}$$

where V is the unit cell volume, j is an index for the lattice modes and Z_k is the effective charge of the kth ion with mass M_k. For the effective charges, there is a sum rule for charge neutrality, i.e. $\Sigma_k(Z_k) = 0$. We note that the effective charge calculated using the above equation is not the same as the ionic charge, the Szigeti charge or the nominal valence charges [30]. In $TbMnO_3$, where the masses of other constituents are much heavier than the oxygen mass, we can neglect the terms other than the terms for oxygen on the left-hand side of eq. (3). The calculated value of the effective charge of oxygen from eq. (3) is the average for all the oxygen sites. Using the observed values of the TO and the LO frequencies in eq. (3) the temperature dependence of the oxygen effective charge (Z_O) is calculated, as shown

in figure 6. The absolute value of Z_{O} is not crucial, what is more important is its change with temperature. We find that Z_{O} increases below T_{N}. If Z_{O} increases, then the induced dipole moment and hence the optical absorption will also increase. The increase in Z_{O} below T_N suggests a change in the bond length between Mn^{3+} cations and the corresponding bond angles, mediated by the O-ions. This result needs to be understood better.

In conclusion, infrared reflectivity measurements of a single crystal of $TbMnO_3$ clearly identify 15 IR active phonon modes. Out of these, three modes show anomalous behaviour below the magnetic phase transition temperature T_{N} which is attributed to spin-phonon coupling. The effective charge of the oxygen ions shows an increase below T_{N}. We hope that our results on phonon softening and an increase in the effective charge of oxygen ions will motivate theoretical studies of phonons in $TbMnO_3$ and their role in the magnetoelectric behaviour.

Acknowledgements

AKS would like to thank the Department of Science and Technology (DST), India, for financial support. Pradeep Kumar would like to thank Council of Scientific and Industrial Research (CSIR), India, for research fellowship.

References

[1] Y Tokura, *Science* **312**, 1481 (2006)
[2] W Eerenstein, N D Mathur and J F Scott, *Nature (London)* **442**, 759 (2006)
[3] C N R Rao and C R Serrao, *J. Mater. Chem.* **17,** 4931 (2007)
[4] S W Cheong and M Mostovy, *Nature Mater.* **6**, 13 (2007)
[5] N A Hill and A Filippetti, *J. Magn. Magn. Mater.* **976**, 242 (2002)
[6] T Kimura, T Goto, H Shintani, K Ishizaka, T Arima and Y Tokura, *Nature (London)* **426**, 55 (2003)
[7] T Goto, T Kimura, G Lawes, A P Ramirez and Y Tokura, *Phys. Rev. Lett.* **92**, 257201 (2004)
[8] Y Yamasaki, H Sagayama, T Goto, M Matsuura, K Hirada and Y Tokura, *Phys. Rev. Lett.* **98**, 147204 (2007)
[9] L M Carron, A de Andres, M J Martinez Lope, M T Casais and J A Alonso, *Phys. Rev.* **B66**, 174303 (2002)
[10] W Wei-Ran, X D Peng and S W Hui Chin, *Phys. Lett.* **22**, 705 (2005)
[11] M N Iliev, M V Abrashev, J Laverdiere, S Jandl, M M Gospodinov, Y Q Wang and Y Y Sun, *Phys. Rev.* **B73**, 064302 (2006)
[12] M Bastjan, S G Singer, G Neuber, S Eller, N Aliouane, D N Argyrion, S L Cooper and M Rubhausen, *Phys. Rev.* **B77**, 193105 (2008)
[13] S Greenwald and J S Smart, *Nature (London)* **166**, 523 (1950)
[14] J S Smart and S Greenwald, *Phys. Rev.* **82**, 113 (1951)
[15] A Pimenov, A A Mukhin, V Yu Ivanov, V D Travkin, A M Balbashov and A Loidl, *Nature Phys.* **2**, 97 (2006)
[16] R V Aguilar, A B Sushkov, C L Zhang, Y J Choi, S W Cheong and H D Drew, *Phys. Rev.* **B76**, 060404 (2007)

[17] Y Takahashi, N Kida, Y Yamasaki, J Fujioka, T Arima, R Shimano, S Miyahara, M Mochizuki, N Furukawa and Y Tokura, *Phys. Rev. Lett.* **101**, 187201 (2008)
[18] R V Aguilar, M Mostovoy, A B Sushkov, C L Zhang, Y J Choi, S W Cheong and H D Drew, *Phys. Rev. Lett.* **102**, 047203 (2009)
[19] A Pimenov, A Shuvaev, A Loidl, F Schrettle, A A Mukhin, V D Travkin, V Yu Ivanov and A M Balbashov, *Phys. Rev. Lett.* **102**, 107203 (2009)
[20] J Laverdiere, S Jandl, A A Mukhin, V Yu Iyanov, V G Iyanov and M N Iliev, *Phys. Rev.* **B73**, 214301 (2006)
[21] E Granado, A Garcia, J A Sanjurjo, C Rettori and I Torriani, *Phys. Rev.* **B60**, 11879 (1999)
[22] W S Ferreira, J A Moreira, A Almeida, M R Chaves, J P Araujo, J B Oliveira, J M Machado Da Silva, T M Sa, T M Mendonca and P S Carvalho, *Phys. Rev.* **B79**, 054303 (2009)
[23] A Paolone, P Roy, A Pimenov, A Loidl, O K Melnikev and A Ya Shapiro, *Phys. Rev.* **B61**, 11255 (2000)
[24] I S Smirnova, *Physica* **B262**, 247 (1999)
[25] C C Holmes, T Vogt, S M Shapiro, S Wakimoto, M A Subramanian and A P Ramirez, *Phys. Rev.* **B67**, 092106 (2003)
[26] S Tajima, T Ido, S Ishibashi, T Itoh, H Eisaki, Y Mizauo, T Arima, H Takagi and S Uchido, *Phys. Rev.* **B43**, 10496 (1991)
[27] D Meier, N Aliouane, D N Argyriou, J A Mydosh and T Lorenz, *New J. Phys.* **9**, 100 (2007)
[28] P G Klemens, *Phys. Rev.* **148**, 845 (1966)
[29] J F Scott, *Phys. Rev.* **B4**, 1360 (1971)
[30] W Cochran, *Nature (London)* **191**, 60 (1961)